

Broadband Raman amplification in silicon

Daniel R. Solli,^{a)} Prakash Koonath, and Bahram Jalali

Department of Electrical Engineering, University of California, Los Angeles, California 90095, USA

(Received 10 July 2008; accepted 20 September 2008; published online 12 November 2008)

Raman gain is a useful nonlinear phenomenon that has made optically pumped silicon lasers and amplifiers a reality. Unfortunately, the bandwidth of Raman gain in silicon is normally rather limited, owing to the narrow Raman linewidths typical of crystalline materials. Here, we report Raman amplification in silicon with a spectrum that is modified by the simultaneous occurrence of self-phase-modulation. This combined nonlinear action produces a broad Raman gain spectrum from a narrowband pump source. © 2008 American Institute of Physics. [DOI: 10.1063/1.3005408]

The observation of stimulated Raman scattering (SRS) in silicon waveguides¹ has proven that silicon is a bonafide optical gain medium. Since then, high-gain Raman amplifiers have been demonstrated,^{2,3} and silicon lasers have been constructed for pulsed⁴ and continuous-wave operation.⁵ Unfortunately, silicon has a narrow Raman linewidth,⁶ which restricts the bandwidth of silicon Raman amplifiers and limits their range of practical applications. Recently, in pioneering experiments, broadband parametric gain based on phase-matched four-wave mixing was demonstrated in silicon waveguides.⁷ In contrast to Raman gain, however, this mechanism requires phase matching, which necessitates careful control of the waveguide dimensions or application of external stress.

Researchers have also attempted to coax silicon into a different type of light emission—optical continuum generation. The goal of this effort is to produce broadband light from a narrowband input for chip-scale optical signal processing.^{8–11} The generation of continuum in silicon is complicated by two-photon absorption (TPA), which rapidly depletes the input light and liberates free carriers that produce their own intensity-dependent absorption and refraction.¹²

In silicon-based continuum generation, self-phase modulation (SPM) broadens the spectrum of the input pulse. Two independent nonlinear effects, Kerr refraction and free-carrier refraction (FCR), produce SPM. The familiar Kerr contribution to the refractive index is electronic in origin and responds to the field essentially instantaneously.¹³ On the other hand, the free-carrier response is cumulative: the generation rate of free carriers produced by TPA is proportional to the square of the intensity,¹⁴ and the refractive index change due to these carriers is proportional to their density. Since carriers typically survive for nanoseconds or longer once created, their decay is usually negligible within individual picosecond pulses.

In this paper, we demonstrate Raman scattering with simultaneous continuum generation in a silicon waveguide to produce broadband gain (significantly larger than the natural Raman linewidth of the medium). Being a Raman process, broadband gain is produced here without the need for any phase matching. Using picosecond pump pulses, we show that the broadband Raman gain spectrum displays characteristic features of SPM from both Kerr refraction and FCR. We

are able to alter the shape of the gain spectrum by adjusting the properties of the pump pulse and its timing relative to the Stokes probe.

Our Raman pump pulses are generated from a mode-locked laser producing near-transform-limited picosecond pulses at 1550 nm (3 dB width of ~ 2 nm). These pulses are amplified with low nonlinear distortion using chirped pulse amplification (CPA). By controlling the stretch-to-compression ratio in the CPA setup, we produced two different chirped pulses of approximately 3 and 42 ps to demonstrate the ability to tailor the gain spectrum by controlling the pulse duration. The pump was coupled to a silicon waveguide with mode area of roughly $2.8 \mu\text{m}^2$ and length of ~ 1.5 cm. The total insertion loss (coupling plus propagation) of the waveguide was 10 dB. The maximum peak intensity levels coupled to the waveguide were ~ 20 and $\sim 6 \text{ GW/cm}^2$ for the 3 and 42 ps pulses, respectively.

In order to measure the Raman gain spectra, we used a portion of the laser output to generate a pulsed supercontinuum probe spanning >50 nm around the Stokes spectral region, and synchronized it with the pump. Since the probe was broadband, gain spectra could be measured without tuning. Given the Raman shift of silicon,⁶ the expected center wavelength of the Stokes field is ~ 1686 nm for a 1550 nm pump.

In Fig. 1, we show the broadband Raman gain spectra produced by 3 ps pump pulses. These broadened Raman

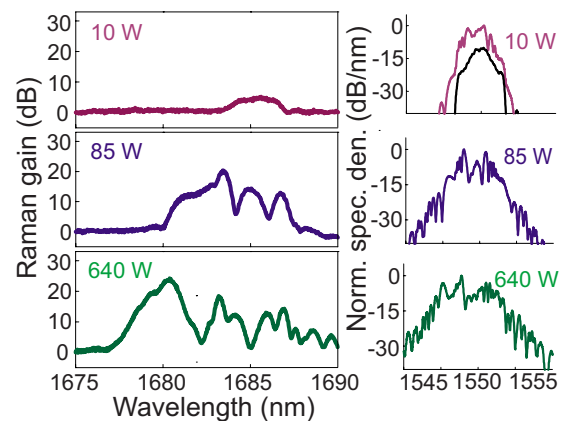


FIG. 1. (Color online) Measured broadband Raman gain spectra with 3 ps pump pulses. (Left) Raman gain spectra produced by pump pulses with the indicated (input) peak power levels. (Right) Normalized spectral densities of pump pulses at the waveguide output.

^{a)}Electronic mail: solli@ucla.edu.

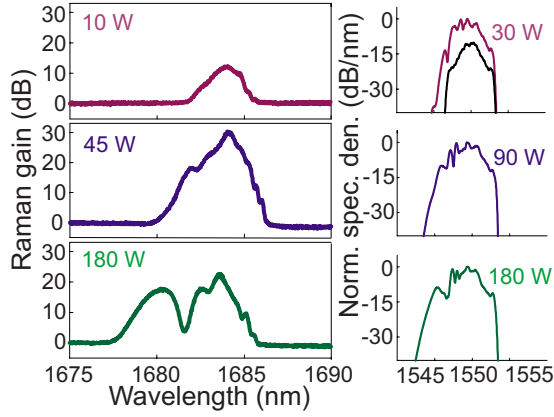


FIG. 2. (Color online) Measured broadband Raman gain spectra with 42 ps pump pulses. (Left) Raman gain spectra produced by pump pulses with the indicated (input) peak power levels. (Right) Normalized spectral densities of pump pulses at the waveguide output.

spectra show rapid undulations characteristic of SPM and are shifted toward blue wavelengths due to FCR, as will be discussed below. We point out that the natural Raman linewidth in silicon is ~ 1 nm. For reference, we also show the broadened pump spectra at the waveguide output for different peak power levels.

Figure 2 shows the Raman gain spectra produced by 42 ps pulses. In this case, the Raman spectrum is also broadened and blueshifted but remains relatively smooth compared with the Raman spectrum produced by the shorter pulses. In addition, the majority of the gain is shifted to wavelengths shorter than 1686 nm, even for fairly modest pump power. At higher power, the gain spectrum develops a second lobe appearing further to the blue. It is worth noting that for a given power level, the longer pulses generate more carriers than the shorter pulses, which indicates a stronger influence of free-carrier absorption (FCA), particularly on the trailing edge of the pulse. This occurs because the carrier density depends on the time integral of the square of the intensity, whereas the instantaneous frequency shift caused by FCR depends on the momentary value of the intensity squared.⁸ Thus, determining the relative influence of FCR and FCA for different pulse durations and peak power levels is not entirely straightforward.

Intuitively, one may expect the Raman spectrum to closely resemble the output pump spectrum. Although they have some similarities, fine spectral features in the pump tend to wash out in the gain spectrum because of convolution with the intrinsic Raman linewidth of the medium. In addition, the pump evolution and Raman gain are distributed throughout the propagation; thus, the Raman profile is a cumulative reflection of this process rather than a simple replica of the final pump spectrum. Nevertheless, it is important to develop a qualitative understanding of the spectral evolution of the pump to account for certain characteristics of the gain spectrum.

The effect of the free-carrier and Kerr nonlinearities on the pump can be qualitatively understood by considering their tandem actions. The dynamic phase shift imparted by Kerr refraction upshifts the frequency of the pulse's trailing edge and downshifts the leading edge.¹³ Carrier refraction, however, upshifts both the leading and trailing slopes.¹² Thus, FCR partially negates the Kerr redshift on the leading edge but adds to the blueshift on the trailing side.¹² On the

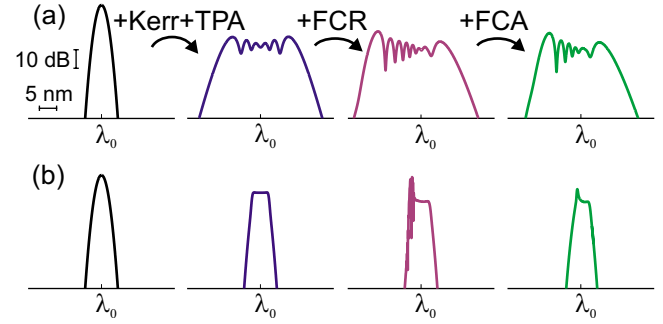


FIG. 3. (Color online) Impact of nonlinearities on the pulse spectrum in a silicon waveguide: (a) 3 ps, 640 W and (b) 42 ps, 180 W. Left to right: input spectrum; output spectrum with the action of Kerr nonlinearity and TPA; output spectrum with the action of Kerr, TPA, and FCR; output spectrum with the action of Kerr, TPA, FCR, and FCA.

other hand, FCA preferentially attenuates the trailing half of the pulse, absorbing the new blue frequency components on this side. The net result is still a broadened, blueshifted pulse, but its spectral extent is limited to some degree by the combined nonlinearities.¹²

The pump spectral modifications depend on the temporal duration of the starting pulse. Figure 3 illustrates the effects of the different nonlinearities for 3 and 42 ps pulses. These changes are derived from our numerical simulations, which are described below. For the shorter pulses, the pump spectrum is marked by deep undulations; however, for the 42 ps pulses, much of the spectrum is relatively smooth except for a sharp blueshifted feature produced by FCR. This feature leads to a blueshifted lobe in the Raman spectrum. When transferred to the Raman spectrum, however, the lobe is smoother because of convolution with the Raman linewidth.

To study the properties of the broadened Raman spectra, we have conducted numerical simulations of SRS (pump + input Stokes pulses) in silicon waveguides using the generalized nonlinear Schrödinger equation for the field envelope,

$$\frac{\partial A(z,t)}{\partial z} + \frac{i\beta_2}{2} \frac{\partial^2 A(z,t)}{\partial t^2} = i\gamma \left[1 + \frac{i}{\omega_0} \frac{\partial}{\partial t} \right] \times A(z,t) \int_{-\infty}^t R(t-t') |A(z,t')|^2 dt' + \left(\frac{i\omega_0 n_{\text{FCR}}}{c} - \frac{1}{2} \alpha_{\text{FCA}} \right) A(z,t),$$

where $D = -9.5$ fs/nm cm describes the dispersion of bulk silicon ($\beta_2 = -\lambda^2 D / 2\pi c$), γ is the nonlinear coefficient, and α_{FCA} and n_{FCR} account for FCA and FCR. The nonlinear coefficient is given by $\gamma = \omega_0 n_2 / c A_{\text{eff}} + i\beta_{\text{TPA}} / 2A_{\text{eff}}$, where $n_2 = 6 \times 10^{-5}$ cm²/GW, A_{eff} is the mode area, and the TPA coefficient is $\beta_{\text{TPA}} = 0.5$ cm/GW. This prescription is described in Ref. 10; however, in the present case, FCR is included. The function $R(t)$ includes the instantaneous (electronic) and the delayed (Raman) nonlinear responses. For narrowband signals, SRS can be modeled as direct amplification, but the present approach is needed for broadband fields.^{15,16} We assume a Raman gain coefficient of ~ 7 cm/GW on resonance, which is conservatively within the range of published values^{1,2} and a linewidth of 105 GHz.⁶ Coherent four-wave mixing, which has both Raman-resonant and broadband electronic contributions, is

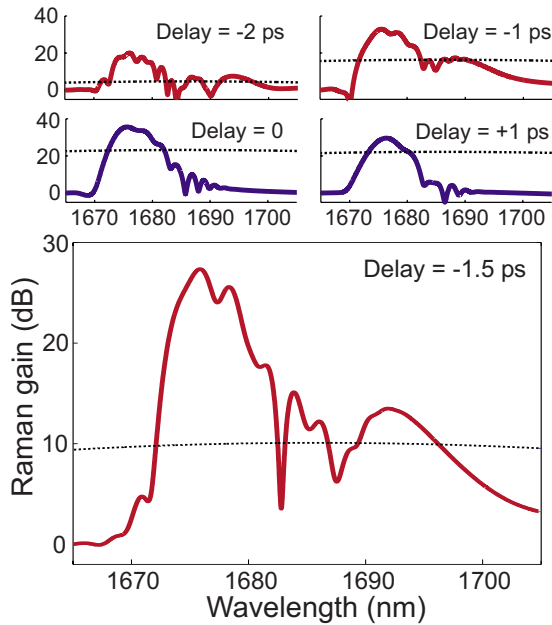


FIG. 4. (Color online) Simulated Raman gain spectra at the indicated pump-probe delay (pump: ~ 3 ps, 640 W). Negative delay corresponds to probe on the leading slope of pump. Dotted lines mark “break-even” levels for the pump on/off gain. For -1.5 ps delay, the on/off gain is largest, and the spectral shape resembles that measured experimentally.

automatically included in the model but does not have a significant impact on the amplified Stokes signal.

In order to determine the FCA and FCR, the concentrations of free electrons and holes are calculated using the independent differential equation that describes free-carrier generation from TPA: $\partial N_{e=h}(z, t)/dt = \beta_{\text{TPA}}|A(z, t)|^4/2h\omega_0 A_{\text{eff}}$. We then calculate α_{FCA} and n_{FCR} using the following empirical formulas: $n_{\text{FCR}} = -(8.8 \times 10^{-22} N_e + 8.5 \times 10^{-18} N_h^{0.8})$ and $\alpha_{\text{FCA}} = 8.5 \times 10^{-18} N_e + 6.0 \times 10^{-18} N_h$, where N_e and N_h are the densities of electrons and holes in units of cm^{-3} . These formulas were obtained by the study of doped silicon but are also widely used for optically produced carriers.^{17,18} We note that the optical properties of the carriers are not fully understood, particularly for high intensities, and certain physical parameters (e.g., silicon’s Raman gain coefficient) are not precisely known. Thus, the modeling is primarily intended to develop a qualitative understanding.

The simulations produce broadband Raman gain spectra and also reveal that the relative delay between the pump and Stokes pulses can be used to control the gain profile. Figure 4 shows a family of simulated gain spectra obtained by varying the initial delay between the pulses. As broadband carrier losses increase toward the trailing edge of the pump, the gain

relative to the output Stokes level without the pump (on/off gain) tends to be larger on the leading edge of the pulse. We also observe that when the probe is timed on the pump’s leading edge, the gain develops a multipeak structure, similar to what is observed experimentally. It is also important to note the role of silicon’s dispersion: in 1 cm of travel, pump and probe pulses with an ~ 100 nm wavelength separation will experience a walk off of ~ 1 ps. The redshifted probe overtakes the pump pulses, influencing the gain profile. On the other hand, the gain is stronger earlier in the propagation before TPA and FCA deplete the pump.

In conclusion, we have observed simultaneous spectral broadening and Raman gain in a silicon waveguide, which significantly extends its amplification bandwidth beyond the intrinsic Raman linewidth. Since the nonlinear dynamics depends on the pulse characteristics (i.e., pulse power, chirp, duration, and timing), the gain spectrum can also be tuned and shaped. The ability to produce a broadened gain spectrum with a tailored profile in silicon may be very useful for on-chip optical signal processing and producing tunable silicon lasers.

This work was supported by the DARPA EPIC programs.

- ¹R. Claps, D. Dimitropoulos, V. Raghunathan, Y. Han, and B. Jalali, *Opt. Express* **11**, 1731 (2003).
- ²Q. Xu, V. R. Almeida, and M. Lipson, *Opt. Express* **12**, 4437 (2004).
- ³V. Raghunathan, O. Boyraz, and B. Jalali, 2005 Conference on Lasers and Electro-Optics, CMU1 (unpublished), Vol. 1, p. 349.
- ⁴O. Boyraz and B. Jalali, *Opt. Express* **12**, 5269 (2004).
- ⁵H. Rong, R. Jones, A. Liu, O. Cohen, D. Hak, A. Fang, and M. Paniccia, *Nature (London)* **433**, 725 (2005).
- ⁶P. A. Temple and C. E. Hathaway, *Phys. Rev. B* **7**, 3685 (1973).
- ⁷M. A. Foster, A. C. Turner, J. E. Sharping, B. S. Schmidt, M. Lipson, and A. L. Gaeta, *Nature (London)* **441**, 960 (2006).
- ⁸O. Boyraz, P. Koonath, V. Raghunathan, and B. Jalali, *Opt. Express* **12**, 4094 (2004).
- ⁹E. Dulkeith, Y. A. Vlasov, X. Chen, N. C. Panoiu, and R. M. Osgood, *Opt. Express* **14**, 5524 (2005).
- ¹⁰L. H. Yin, Q. Lin, and G. P. Agrawal, *Opt. Lett.* **32**, 391 (2007).
- ¹¹P. Koonath, D. R. Solli, and B. Jalali, *Appl. Phys. Lett.* **91**, 061111 (2007).
- ¹²P. Koonath, D. R. Solli, and B. Jalali, *Appl. Phys. Lett.* **93**, 091114 (2008).
- ¹³G. P. Agrawal, *Nonlinear Fiber Optics*, 4th ed. (Academic, San Diego, 2007).
- ¹⁴K. W. DeLong, A. Gabel, C. T. Seaton, and G. I. Stegeman, *J. Opt. Soc. Am. B* **6**, 1306 (1989).
- ¹⁵X. Chen, N. C. Panoiu, and R. M. Osgood, *IEEE J. Quantum Electron.* **42**, 160 (2006).
- ¹⁶Q. Lin, O. J. Painter, and G. P. Agrawal, *Opt. Express* **15**, 16604 (2007).
- ¹⁷A. Irace, G. Breglio, M. Iodice, and A. Cutolo, in *Silicon Photonics*, Topics in Applied Physics Vol. 94, edited by L. Pavesi and D. J. Lockwood (Springer, Berlin, 2004), p. 361.
- ¹⁸R. A. Soref and B. R. Bennett, *IEEE J. Quantum Electron.* **QE-23**, 123 (1987).